arXiv:2610.37509v2 [cs.RO] 28 Oct 2026

Ego-CEVR: Learning Cross-Embodiment Visual Representations from Human Egocentric Videos

Keru Zhou[1,2], **Zhirui Fang**[3], **Xinrun Xu**[2], **Yaopeng Lou**[4], **Zeyuan He**[5], **Zihao Zhu**[1], **Xinze Niu**[1], **Chen Wang**[1], **Tianfu Li**[1], **Samith Va**[2], **Xiyue Zhang**[6], **Bin Qian**[2], **Junwei Li**[2], **Wenjia Ding**[7], **Yicheng Xu**[1], **Bowen Jiang**[1], **Wenhao Wang**[1], **Ziwei Wang**[3], **Chang Zhou**[1,†], **Li Liu**[1], **Xiu Li**[2,*], **Maoqing Yao**[1,*]

[1]Maniformer
[2]Tsinghua University
[3]Nanyang Technological University
[4]Huazhong University of Science and Technology
[5]The Chinese University of Hong Kong, Shenzhen
[6]Zhejiang University
[7]Harbin Institute of Technology

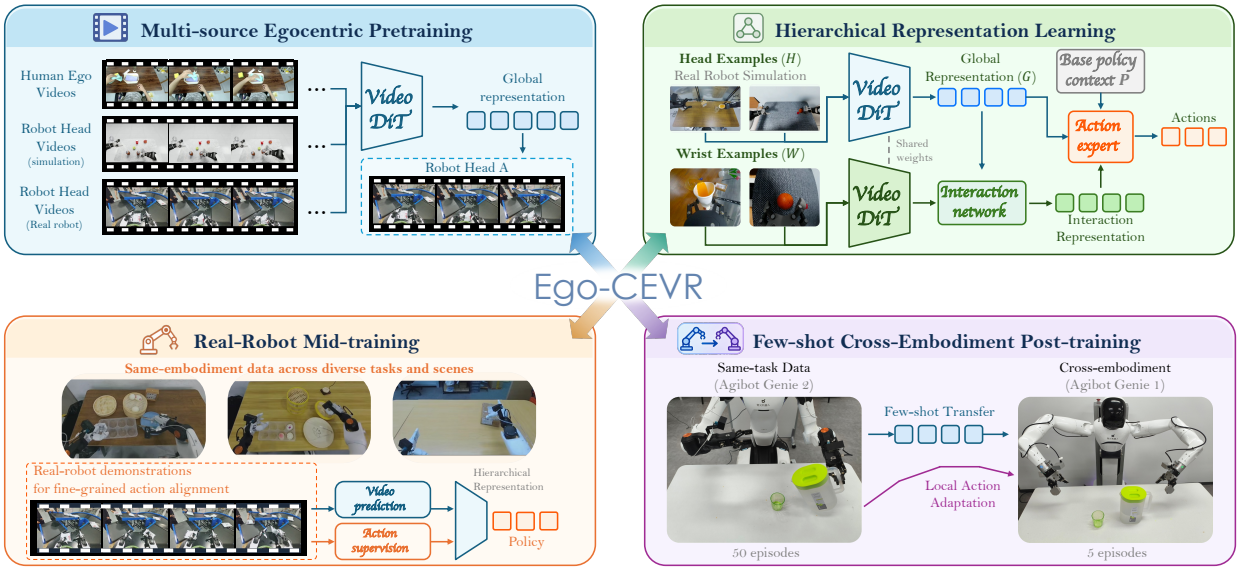

Figure 1: **Ego-CEVR.** Hierarchical representation learning links global task representations learned from egocentric video to local interaction representations grounded in wrist observations and robot actions. Multi-source egocentric pretraining learns the global representation from human and robot videos. Real-robot mid-training uses demonstrations across tasks and scenes from a single robot embodiment to align the representations with fine-grained actions. Few-shot post-training uses demonstrations of the same task from a new robot embodiment to adapt the policy across embodiments.

*Corresponding authors: Xiu Li and Maoqing Yao.
†Project leader: Chang Zhou.

Abstract

As egocentric video becomes increasingly available for embodied learning, an important research question is how to turn this low-cost, scalable source of data into robot manipulation capabilities. Egocentric videos naturally provide rich context for high-level task understanding, while real-robot demonstrations with wrist observations and action annotations provide supervision for fine-grained action alignment. We present Ego-CEVR, a data-native framework for hierarchical visual representation learning that assigns distinct learning objectives to global and interaction representations. The global module learns object relations, task state, and temporal progress through future prediction on egocentric video. The interaction module interprets wrist observations in global context and learns local alignment and contact cues through robot action supervision. Separate residual paths expose both representations to the action policy, preserving direct access to task context alongside fine-grained execution information. Ego-CEVR supports independent pretraining of its global video module on large-scale egocentric videos and videos from diverse robot embodiments, without requiring robot action labels or paired wrist observations.

1 Introduction

In recent years, a series of works [1–4] and their applications have marked the rapid development of embodied manipulation. More and more embodied data from various sources such as egocentric video (Ego), Universal Manipulation Interface (UMI) and cross embodiments data have been applied to the training of models.[5–7] As embodied data scale up, different types of data are expected to play distinct roles in robot learning.[8] An important challenge is to systematically use data from diverse sources with varying forms of supervision. [9–11]. However, how can we design data-native models that are specifically tailored to these various data sources in order to make better use of the data from these different sources? This issue has not yet been fully discussed.

VLA policies transfer visual and linguistic priors to robot control, yet semantic generalization does not always translate into faithful execution on unseen tasks [12–14]. Predictive world models learn how scenes evolve during manipulation, but using this knowledge for precise local control remains challenging [15–17]. Integrating semantic understanding, world modeling, and action generation is therefore a promising direction [18, 19]. To benefit from heterogeneous video and robot data, such integration must also specify which representations can be learned without actions and how robot supervision should ground them in local control.

Reusing manipulation experience from humans or other robots requires handling differences in morphology, action space, and local interaction geometry [20, 21]. Despite differences in embodiment, similar manipulation tasks often involve similar changes in the spatial and functional relationships between objects. Egocentric videos and robot head-camera videos can therefore both provide supervision for learning task-level visual representations [5, 22]. Wrist observations provide a closer view of the end effector and its target, revealing local cues for action alignment and contact. Video prediction alone may not sufficiently ground these cues in robot actions. We therefore learn global task context through video prediction and local interaction representations through robot action supervision.

Following this principle, we introduce **Ego-CEVR**, a data-native framework for hierarchical visual representation learning (Figure 2). It learns global task context from human egocentric and robot head-camera videos through future prediction, and learns local interaction representations from wrist observations under robot action supervision. Wrist features query the global representation, establishing a hierarchy in which local interaction draws on task context while the global representation is computed independently of the interaction module.

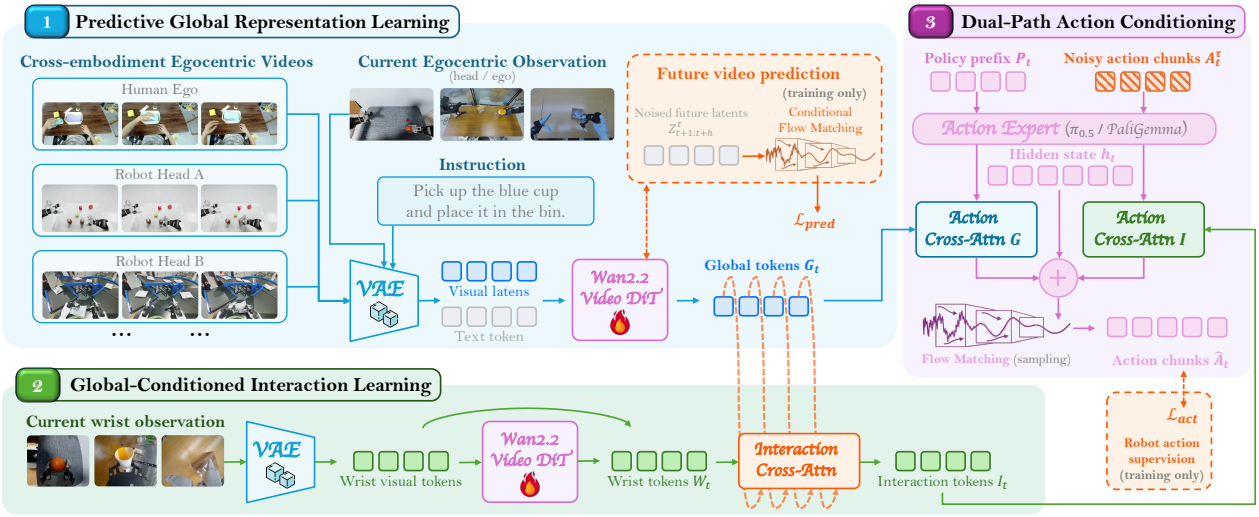

Figure 2: **Ego-CEVR architecture.** Future-video prediction supervises global tokens extracted from the current ego or head observation. Wrist tokens query global tokens to form interaction tokens. The action expert receives both token sets through separate residual cross-attention paths, alongside the base policy prefix. Future-video prediction is used during training; inference uses current observations without generating future video.

Experiments on LIBERO [23], LIBERO-Plus [24], RoboTwin 2.0 [25], and real robots show improvements in task success and robustness. Ablations further examine the contributions of hierarchical representation learning and multi-source video pretraining.

Our main contributions are:

- We propose a data-native framework that incorporates multi-source egocentric videos and action-labeled robot demonstrations at different training stages to learn task-level and local execution knowledge.
- We develop a few-shot cross-embodiment adaptation procedure that combines task knowledge learned from video with a few demonstrations from the target robot.
- We design a hierarchical representation learning architecture that learns distinct yet complementary representations for high-level task understanding and fine-grained action alignment.

2 Related Work

Vision-language-action policies. Vision-language-action (VLA) models transfer pretrained visual and linguistic knowledge to robot control, achieving substantial progress in semantic generalization, multitask manipulation, and deployment across environments [1–4, 26, 27]. However, object recognition and semantic understanding acquired from image-text data do not directly specify how object states should evolve during manipulation or how actions should realize an instruction. On unseen tasks, policies may reproduce familiar training behaviors, causing their execution to deviate from the intended instruction [21]. These limitations motivate incorporating future visual prediction into policy learning, providing temporal supervision through state transitions and enabling learning from video experience beyond action-labeled robot demonstrations [28, 29].

Predictive world models for robot control. Video foundation models provide rich spatiotemporal priors for learning manipulation processes and their visual consequences [30, 31]. Predictive policies guide action generation using future visual states or internal video-model representations, while world-action models further couple visual state evolution with robot actions [15, 16, 21, 32]. These approaches expand the use of video knowledge for control, but visual generation quality does not necessarily ensure the spatial precision required

for fine manipulation. Visually plausible predictions may fail to preserve the relative positions, alignment, and contact relationships needed for accurate execution, and prediction errors can propagate into action errors on unseen tasks and scenes. Consequently, recent work more directly addresses the control relevance of predictive representations. GE-Act 2.0 develops a control-oriented latent space, while VPP2 improves predictive and action generalization through manipulation-video pretraining and subsequent adaptation [17, 33, 34]. Fast-WAM further demonstrates that predictive supervision can shape control representations during training without requiring explicit future-video generation at deployment [35]. These advances raise a central question: how should manipulation knowledge acquired from video be organized into policy conditions that support precise execution?

Integrating vision-language understanding and world modeling. The complementary requirements of task semantics, manipulation dynamics, and local control motivate integrating vision-language understanding, world prediction, and action generation. One line of work jointly models video and actions or coordinates semantic understanding, visual prediction, and control through multiple experts [19, 36–38]. Another incorporates predictive information into VLA policies through future-latent alignment or attention-based conditioning [18, 39, 40]. These studies show that temporal knowledge learned through video prediction can complement the visual-language context of a base policy. For manipulation policies with both Head and Wrist observations, this integration also requires determining the learning roles of different views: how to acquire transferable task knowledge, how embodiment-dependent local interaction should use that knowledge, and how both should support action generation. Ego-CEVR addresses these questions through a representational hierarchy with an explicit conditional dependency. Head video prediction learns global representations, which condition the learning of execution-relevant interaction representations. The action expert accesses both through separate conditioning paths alongside the base-policy context.

Cross-embodiment learning from heterogeneous egocentric data. Human egocentric videos capture diverse object interactions and task variations, providing coverage that is difficult to obtain through robot teleoperation alone. Early work uses such videos to learn transferable visual representations and rewards [41, 42]. Subsequent methods transfer human manipulation experience to robot policies through human-robot data alignment, hand-motion estimation, or action retargeting [5, 43, 44]. These approaches demonstrate the value of human experience, while their motion-estimation and alignment requirements also affect the range of usable data and the quality of available supervision. EgoWAM and Ego4WAM further investigate how prediction targets, data alignment, and supervision influence transfer, showing that video-only supervision can provide an effective foundation for subsequent robot learning [22, 45]. These findings highlight the need to match model learning objectives to the observations and supervision available across data sources. Ego-CEVR incorporates this requirement into a shared Head/Ego video learning interface spanning humans and heterogeneous robot embodiments. The global module supports independent learning without a common action space or paired Wrist observations, while robot demonstrations ground the learned knowledge in local interaction and the target robot's action mapping.

3 Method

3.1 Overview and Data Formulation

We use egocentric data to refer to first-person videos from either humans or robots. When the source needs to be specified, we use human egocentric videos and robot head-camera videos, respectively. Both are captured with non-fisheye RGB cameras. For egocentric data, only the first-person camera view is used, without paired wrist observations or robot action annotations. Real-robot demonstrations, in contrast, include observations from a head camera and two wrist cameras, together with robot action annotations. We denote the egocentric observation at time t by I_t^H and the pair of wrist observations by I_t^W. The action sequence used for policy training is denoted by A_t. We use ℓ for the language instruction when describing the language-conditioned modules below.

As illustrated in Figure 2, Ego-CEVR consists of a global video representation module, an interaction representation module, and a representation-augmented action expert. The global module learns from

egocentric video through future prediction and produces a representation G_t. The interaction module uses wrist observations and G_t to produce an interaction representation I_t under robot action supervision. The global module can therefore be pretrained on egocentric data independently of wrist observations and action annotations.

We use $\pi_{0.5}$ [4] as the base policy and retain its original encoding of observations, language instructions, and robot state. Two additional attention branches provide G_t and I_t to the action expert. The following subsections describe the representation learning objectives and action conditioning in detail.

3.2 Predictive Global Representation Learning

We use the diffusion transformer (DiT) [46] of the pretrained Wan2.2 video model [30, 47] as our visual backbone. Given the current egocentric observation I_t^H and language instruction ℓ, a frozen VAE encoder E maps the observation to a latent $z_t = E(I_t^H)$. The language-conditioned video DiT processes z_t at a zero noise timestep. We extract attention value tokens from selected intermediate layers and concatenate them along the token dimension to form the global representation G_t. The resulting tokens retain spatial information from these layers for interaction modeling and action prediction. At inference, extracting G_t does not require generating future video.

We supervise the video backbone through conditional flow matching [48] over future video latents. The frozen VAE encoder E maps the current egocentric frame to z_t and the subsequent video frames to future latents $Z_{t+1:t+h}$, where h denotes the prediction horizon in latent timesteps. During training, we keep z_t clean and construct noisy future latents through linear interpolation:

$$Z^{\tau}_{t+1:t+h} = (1-\tau)Z_{t+1:t+h} + \tau\epsilon, \qquad \epsilon \sim \mathcal{N}(0, I), \quad \tau \in [0, 1]. \tag{1}$$

Given the noisy future latents $Z^{\tau}_{t+1:t+h}$ and noise timestep τ, the video DiT predicts the vector field u_v, conditioned on z_t and the language instruction ℓ. The prediction objective is

$$\mathcal{L}_{\text{pred}} = \mathbb{E}_{\tau,\epsilon}\left[w(\tau)\ \text{MSE}\left(u_v,\ \epsilon - Z_{t+1:t+h}\right)\right], \tag{2}$$

where $w(\tau)$ is the timestep-dependent loss weight, and the mean squared error is computed only over valid future latent positions. By modeling visual changes during manipulation, $\mathcal{L}_{\text{pred}}$ trains the video backbone to produce global representations from current egocentric observations.

The video backbone can be pretrained independently of the interaction module and action policy using human egocentric videos and robot head-camera videos. This stage requires video and corresponding text conditions, but no shared robot action space. During pretraining, only the video backbone is updated, while the VAE remains frozen. Downstream robot learning can initialize the video DiT either from this stage or directly from the pretrained Wan2.2 weights.

3.3 Global-Conditioned Interaction and Action

Given the current wrist observations I_t^W, we obtain wrist features W_t using the frozen VAE encoder and shared video DiT introduced in the previous section. The wrist observations are processed in a separate forward pass using the same cross-layer feature readout. The interaction network F_I then attends to the global representation G_t to incorporate scene and task context into the wrist features, yielding an interaction representation:

$$I_t = F_I(W_t, G_t). \tag{3}$$

The global representation G_t is computed from the egocentric observation and language instruction without using wrist features. The interaction representation I_t combines wrist features W_t with G_t, allowing local cues for approach, alignment, and contact to be interpreted in the context of the current task and scene.

For action generation, we retain the original conditioning pathway of $\pi_{0.5}$ for current egocentric and wrist observations, the language instruction, and robot state. Let P_t denote the resulting base-policy context. Conditioned on P_t, the action expert processes the noisy action sequence and produces final-layer hidden

states h_t. We augment these states with two independent cross-attention branches that read the global and interaction representations:

$$\widetilde{h}_t = h_t + \alpha \ \mathrm{CrossAttn}_G(h_t, G_t) + \beta \ \mathrm{CrossAttn}_I(h_t, I_t). \tag{4}$$

Both branches use h_t as queries. Their keys and values come from G_t and I_t, respectively. The learnable scaling parameters α and β are initialized to zero. The fused states $\widetilde{h}_t$ are mapped through the original output projection to the action vector field u_a, and action sequences are generated using the flow-matching sampling procedure of $\pi_{0.5}$.

Following the flow-matching action formulation of $\pi_{0.5}$ [4], we construct the noisy action sequence as

$$A_t^\tau = (1-\tau)A_t + \tau\epsilon_a, \qquad \epsilon_a \sim \mathcal{N}(0, I), \quad \tau \in [0, 1]. \tag{5}$$

Here, A_t is the ground-truth action sequence. The action prediction objective is

$$\mathcal{L}_{\mathrm{act}} = \mathbb{E}_{\tau,\epsilon_a}\left[\mathrm{MSE}\left(u_a(A_t^\tau, \tau \mid P_t, G_t, I_t), \epsilon_a - A_t\right)\right]. \tag{6}$$

This loss trains the action expert and the two attention branches to use the global and interaction representations for action prediction. It also provides action supervision for the interaction network F_I, encouraging I_t to retain information relevant to local execution.

During training on robot demonstrations, we combine action supervision with egocentric video prediction using the overall objective:

$$\mathcal{L}_{\mathrm{total}} = \mathcal{L}_{\mathrm{act}} + \lambda_{\mathrm{pred}}\mathcal{L}_{\mathrm{pred}}, \tag{7}$$

where λ_{pred} controls the relative contribution of the video prediction loss. The action-conditioning representations P_t, G_t, and I_t are constructed from current observations and task conditions, while future egocentric frames are used only to compute $\mathcal{L}_{\mathrm{pred}}$.

4 Experiments

We evaluate our method in simulation and on real world robots. Our simulation experiments use LIBERO [23], LIBERO-Plus [24], and RoboTwin 2.0 [25] to assess manipulation performance, robustness to distribution shifts, and bimanual manipulation, respectively. Controlled ablations examine the contributions of hierarchical representations and view-specific learning objectives. Real-robot experiments use the AgiBot G1 and G2 platforms to evaluate video-guided task transfer and few-shot cross-embodiment adaptation. We further investigate the benefits of human egocentric and robot head-camera videos on Plug Insertion, Water Pouring, and Package Sorting.

4.1 Evaluation Setup

Benchmarks. We evaluate manipulation performance on LIBERO, robustness to perturbations on LIBERO-Plus, and bimanual manipulation under the Easy and Hard settings of RoboTwin 2.0. All evaluations follow the standard protocols of the respective benchmarks, with task success rate (%) as the evaluation metric. For LIBERO-Plus, we evaluate our policy trained on LIBERO.

Comparisons and experimental controls. We compare our method with representative vision-language-action policies and world-model-based manipulation approaches. In controlled ablations, we keep robot demonstrations, camera inputs, base-policy initialization, and evaluation settings consistent to assess the contribution of each design choice. Detailed ablation configurations and transfer settings are described in the corresponding subsections. Implementation details for training and evaluation are provided in the supplementary material.

4.2 Manipulation and Robustness

Table 1: LIBERO success rate (%). Avg. retains the aggregate reported with each result. Bold indicates the best listed score in each column.

Method	Spatial	Object	Goal	Long	Avg.
π_0 [3]	95.8	96.2	**98.8**	85.2	94.2
$\pi_{0.5}$ [4]	98.8	98.2	98.0	92.4	96.9
OpenVLA-OFT [49]	97.9	97.6	98.4	94.5	97.1
VLA-JEPA [40]	96.2	99.6	97.2	**95.8**	97.2
Fast-WAM [35]	98.2	**100.0**	97.0	95.2	97.6
Ego-CEVR (ours)	**99.2**	99.8	98.2	93.6	**97.7**

LIBERO. As shown in Table 1, Ego-CEVR achieves an average success rate of 97.7%, close to the reported results of representative WAMs, including Fast-WAM [35] at 97.6% and VLA-JEPA [40] at 97.2%, while exceeding the 96.9% achieved by the VLA policy $\pi_{0.5}$ [4]. Ego-CEVR achieves the highest success rates among the listed methods on Spatial, reaching 99.2%. It improves over $\pi_{0.5}$ across all four suites, demonstrating competitive performance across different types of in-distribution manipulation tasks.

Table 2: LIBERO-Plus success rate (%) by perturbation type. Average retains each method's reported aggregation and is not recomputed as an unweighted mean of the displayed categories. Bold indicates the best listed score in each column.

Method	Camera	Robot	Language	Light	Background	Noise	Layout	Average
$\pi_{0.5}$ [4]	75.8	79.4	83.3	95.5	95.0	89.6	87.0	85.7
ACoT-VLA [50]	72.6	82.6	87.5	97.7	96.5	87.8	86.6	86.6
VLA-JEPA [40]	63.3	67.1	85.4	95.6	93.6	66.3	85.1	79.5
JEPA-WAM [51]	79.2	59.2	68.2	93.3	94.6	83.6	76.1	79.2
Abot-M0.5 [52]	70.5	**87.4**	**88.6**	94.0	89.7	75.5	85.2	83.4
Being-H0.7 [53]	82.0	59.0	82.8	**97.8**	90.0	93.5	**88.5**	84.8
LingBot-VA [32]	40.9	83.0	86.4	82.3	53.1	64.4	76.2	69.5
cosmos-policy [54]	75.8	63.3	81.7	96.5	88.9	92.7	82.2	82.2
Fast-WAM [35]	17.7	45.3	60.1	52.2	22.8	28.5	61.2	41.3
Ego-CEVR (ours)	**91.1**	78.3	86.6	97.7	**98.8**	**95.4**	85.7	**90.2**

LIBERO-Plus. As shown in Table 2, Ego-CEVR achieves an overall success rate of 90.2%, the highest among the listed methods and 3.6 percentage points above ACoT-VLA, the next-best method overall. It also achieves the highest success rates under camera, background, and noise perturbations, reaching 91.1%, 98.8%, and 95.4%, respectively. In particular, under camera viewpoint perturbations, Ego-CEVR outperforms $\pi_{0.5}$ by 15.3 percentage points, demonstrating improved robustness to camera viewpoint changes. Together with the LIBERO results, these findings show that some WAM baselines achieve high in-distribution success but experience substantial performance degradation under visual perturbations. Ego-CEVR, in contrast, maintains competitive in-distribution performance while achieving better results under multiple types of visual perturbations.

We attribute the advantage under viewpoint perturbations to hierarchical representation learning: the global representation guides the policy toward the correct manipulation goal, while the interaction representation provides local execution cues, enabling precise manipulation under perturbations to the global camera viewpoint. This result is consistent with our design of organizing global manipulation knowledge and local interaction information through hierarchical representation learning.

Table 3: RoboTwin success rate (%) under Easy and Hard conditions. Average retains each method's reported aggregation.

Method	Easy	Hard	Average
$\pi_{0.5}$ [4]	70.7	46.0	58.4
Fast-WAM [35]	77.8	1.9	39.9
UniWAM [19]	75.2	67.6	71.4
WorldScape Policy 2.0 [55]	**84.9**	38.5	61.7
4D-WAM [56]	81.5	41.8	61.6
JEPA-WAM [51]	79.9	36.9	58.4
X-WAM [57]	70.0	25.8	47.9
Abot-M0 [58]	57.4	30.4	43.9
starVLA [59]	46.5	3.2	24.8
GalaxeaVLA [60]	62.7	12.7	37.7
Ego-CEVR (ours)	73.7	**70.7**	**72.2**

RoboTwin 2.0. As shown in Table 3, Ego-CEVR achieves success rates of 73.7% and 70.7% under the Easy and Hard settings, respectively, yielding an average of 72.2%. It achieves the highest average and Hard-setting success rates among the listed methods. Compared with $\pi_{0.5}$, the average and Hard-setting success rates improve by 13.8 and 24.7 percentage points, respectively. From the in-distribution Easy setting to the Hard setting with perturbations such as background and lighting changes, the success rate decreases by only 3.0 percentage points. These results demonstrate that Ego-CEVR maintains high manipulation success under environmental distribution shifts and exhibits out-of-distribution generalization, consistent with the visual robustness observed on LIBERO-Plus.

Overall, Ego-CEVR remains competitive on standard LIBERO tasks and achieves the highest overall success rate on LIBERO-Plus and the highest Hard-setting success rate on RoboTwin 2.0 among the listed methods. We next examine how the hierarchical representation structure and view-specific learning objectives contribute to these results.

4.3 Ablation Study on Hierarchical Representation

We compare Ego-CEVR with two variants: flat feature fusion and a hierarchical model that additionally predicts wrist video. All three settings use the same video sources and robot demonstrations. The results are shown in Table 4.

Hierarchical representation structure. Compared with flat feature fusion, Ego-CEVR improves the average success rate from 96.9% to 97.7% on LIBERO and from 73.8% to 90.2% on LIBERO-Plus, with an improvement of approximately 16.4 percentage points on the latter. Under camera viewpoint perturbations, success increases from 66.7% to 91.1%, a gain of 24.4 percentage points. The larger gain on LIBERO-Plus suggests that hierarchical representations contribute to robustness under perturbations. We attribute this advantage to hierarchical representation learning: the global representation provides task goals and scene context, while the interaction representation learns local execution cues conditioned on this context. These results are consistent with our design of organizing global manipulation knowledge and local interaction information through hierarchical representation learning.

View-specific learning objectives. We extend the video prediction objective from the Head view to both Head and Wrist views. Joint prediction achieves an average success rate of 97.9% on LIBERO, comparable to 97.7% for Ego-CEVR, but lowers the LIBERO-Plus average from 90.2% to 87.4%. This suggests that adding Wrist video prediction may hurt robustness under perturbations. One possible explanation is that wrist-camera motion and rapid changes in the visible region encourage overfitting to view-specific appearance

Table 4: Ablations of representation structure and predictive supervision with matched video sources and robot demonstrations. Results are success rates (%).

Method	LIBERO					LIBERO-Plus							
	Spatial	Object	Goal	Long	Avg.	Camera	Robot	Language	Light	Background	Noise	Layout	Average
$\pi_{0.5}$ [4]	98.8	98.2	98.0	92.4	96.9	75.8	**79.4**	83.3	95.5	95.0	89.6	**87.0**	85.7
Fast-WAM [35]	98.2	**100.0**	97.0	**95.2**	97.6	17.7	45.3	60.1	52.2	22.8	28.5	61.2	41.3
Flat fusion + Head prediction	98.4	98.2	97.0	94.0	96.9	66.7	63.2	77.9	81.1	80.2	71.4	80.6	73.8
Hierarchy + Head/Wrist prediction	**99.4**	99.6	98.0	94.4	**97.9**	88.8	70.8	84.9	96.6	97.4	92.2	86.1	87.4
Hierarchy + Head prediction (Ego-CEVR)	99.2	99.8	**98.2**	93.6	97.7	**91.1**	78.3	**86.6**	**97.7**	**98.8**	**95.4**	85.7	**90.2**

changes, weakening generalization. These results support using video prediction to learn global context from head observations and robot action supervision to learn interaction representations from wrist observations.

4.4 Ego and Cross-Embodiment Knowledge Transfer

Table 5: Video-source ablations on three real-robot manipulation tasks. All settings use the same robot demonstrations for policy training. Results are success rates (%).

Video source	Plug Insertion	Water Pouring	Package Sorting
Robot Head only	20	60	60
Robot Head + 10 h Robot Head	35	95	85
Robot Head + 10 h Human Ego	30	75	80

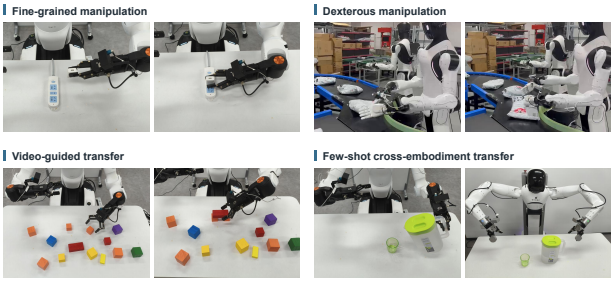

Figure 3: **Real-robot experiments.** Examples of fine-grained and dexterous manipulation, video-guided task transfer, and few-shot cross-embodiment transfer.

Learning from different video sources. To validate the transfer of manipulation knowledge from human egocentric videos to robot control, we conduct experiments on Plug Insertion, Water Pouring, and Package Sorting. Representative real-robot tasks and transfer settings are shown in Figure 3. The *Robot Head only* baseline uses robot head-camera videos extracted from 50 real-robot demonstrations. The two augmented settings add 10 hours of robot head-camera videos or human egocentric videos, respectively.

As shown in Table 5, the *Robot Head only* baseline achieves success rates of 20.0%, 60.0%, and 60.0% on Plug Insertion, Water Pouring, and Package Sorting, respectively. Adding robot head-camera videos improves these rates to 35.0%, 95.0%, and 85.0%, showing consistent gains from additional video data. With the same video duration, human egocentric videos achieve 30.0%, 75.0%, and 80.0%. On Package Sorting, which uses a five-finger dexterous hand, the result with human videos is close to that with robot videos. These results suggest that predictive video learning can transfer manipulation knowledge from human egocentric videos to robot control. In particular, the benefit is most pronounced on the task performed with a five-finger dexterous hand.

Video-guided task transfer. We evaluate cross-task generalization from *Water Pouring* (Task 1) to *Block Stacking* (Task 2) on G2. The base policy is trained on 50 G2 demonstrations of Task 1. We then

Table 6: Task and robot transfer results. Task 1 is *Water Pouring*, and Task 2 is *Block Stacking*. SR denotes success rate (%).

Video-guided task transfer

Evaluation task	G2 Task 1 Full			
	None	Ego Task 2	G2 Task 2 Head	G2 Task 2 Full
G2 Task 1 SR	60	65	65	75
G2 Task 2 SR	0	10	20	55

Few-shot cross-embodiment transfer

Evaluation task	G2 Task 1 Full + Few Shot G1 Task 1			
	None	Ego Task 1	G1 Task 1 Head	G1 Task 1 Full
G2 Task 1 SR	60	65	65	65
G1 Task 1 SR	5	15	35	60

compare adding human egocentric videos of Task 2, G2 head-camera videos of Task 2, or 50 G2 action-labeled demonstrations of Task 2.

As shown in the upper panel of Table 6, the policy has a 0.0% success rate on Task 2 without additional data. Human egocentric videos increase this to 10.0%, and G2 head-camera videos increase it to 20.0%. Both video settings also raise Task 1 success from 60.0% to 65.0%. These results suggest that pretraining on human egocentric videos can transfer task-level semantic understanding to robot control for the new task.

Few-shot cross-embodiment transfer. We evaluate adaptation of Task 1 from G2 to G1. The base training data contain 50 G2 demonstrations and five G1 demonstrations of the same task. We compare adding human egocentric videos or G1 head-camera videos of Task 1 while keeping the five G1 demonstrations fixed. A fully supervised reference uses 50 G1 demonstrations.

As shown in the lower panel of Table 6, the initial policy succeeds on G1 in 5.0% of trials. Human egocentric videos increase this rate to 15.0%, and G1 head-camera videos increase it to 35.0%; the fully supervised reference reaches 60.0%. Success on G2 also rises from 60.0% to 65.0% in both video settings. The few G1 demonstrations provide action supervision for aligning video-learned representations with fine-grained actions on the target robot. With this supervision, both human egocentric and G1 head-camera videos improve generalization to G1. These results show that human and robot egocentric video can support the transfer of manipulation knowledge across embodiments.

5 Discussion and Limitations

The need for data-native models. Our experiments show that different embodied data sources provide different kinds of information for robot learning. This suggests that how a model organizes data and assigns learning objectives may set a limit on what it can learn as data scale grows. The embodied AI industry has accumulated substantial amounts of data, and making effective use of these diverse sources will remain an important challenge. We argue that embodied algorithms should be reconsidered from the perspective of data. Diverse data sources require data-native models designed to learn from different observations and forms of supervision.

Scaling and hierarchical training. As embodied data scale up, larger models are expected to learn from increasingly diverse experience. Yet effective scaling across these data sources remains unresolved. This raises a further question of whether action-aligned supervision alone can lead to emergent capabilities, as observed in LLMs. If video generation scales successfully, transferring knowledge from egocentric video to fine-grained robot actions will still require a distinct stage of representation learning for action alignment. We therefore believe that multistage hierarchical training will become an important direction for embodied learning.

Limitations and future work. Due to resource constraints, we did not pretrain on large-scale human egocentric video or conduct large-scale experiments with different data and model sizes. Whether the proposed framework continues to benefit from substantially larger video collections and exhibits scaling behavior remains an open question.

6 Conclusion

We presented Ego-CEVR, a data-native framework that learns complementary global and interaction representations from video prediction and robot action supervision. Across simulation and real-robot experiments, Ego-CEVR achieves competitive manipulation performance and improved robustness under visual perturbations. Ablations show the benefit of hierarchical representations and of assigning different learning objectives to head and wrist observations. On real robots, additional human egocentric videos improve manipulation performance and support transfer to a new task, while a few-shot demonstrations enable video-learned knowledge to be aligned with fine-grained actions on a new robot. Learning from human egocentric videos and videos from other robots share a common principle, because human-to-robot learning is itself a form of cross-embodiment knowledge transfer.

References

[1] Brianna Zitkovich, Tianhe Yu, Sichun Xu, Peng Xu, Ted Xiao, Fei Xia, Jialin Wu, Paul Wohlhart, Stefan Welker, Ayzaan Wahid, et al. RT-2: Vision-Language-Action Models Transfer Web Knowledge to Robotic Control. In *Conference on robot learning*, pages 2165–2183. PMLR, 2023.

[2] Moo Jin Kim, Karl Pertsch, Siddharth Karamcheti, Ted Xiao, Ashwin Balakrishna, Suraj Nair, Rafael Rafailov, Ethan Foster, Grace Lam, Pannag Sanketi, et al. OpenVLA: An Open-Source Vision-Language-Action Model. *arXiv preprint arXiv:2406.09246*, 2024.

[3] Kevin Black, Noah Brown, Danny Driess, Adnan Esmail, Michael Equi, Chelsea Finn, Niccolo Fusai, Lachy Groom, Karol Hausman, Brian Ichter, et al. π_0: A Vision-Language-Action Flow Model for General Robot Control. *arXiv preprint arXiv:2410.24164*, 2024.

[4] Physical Intelligence, Kevin Black, Noah Brown, James Darpinian, Karan Dhabalia, Danny Driess, Adnan Esmail, Michael Equi, Chelsea Finn, Niccolo Fusai, et al. $\pi_{0.5}$: a Vision-Language-Action Model with Open-World Generalization. *arXiv preprint arXiv:2504.16054*, 2025.

[5] Simar Kareer, Dhruv Patel, Ryan Punamiya, Pranay Mathur, Shuo Cheng, Chen Wang, Judy Hoffman, and Danfei Xu. EgoMimic: Scaling Imitation Learning via Egocentric Video. In *2025 IEEE International Conference on Robotics and Automation (ICRA)*, pages 13226–13233. IEEE, 2025.

[6] Cheng Chi, Zhenjia Xu, Chuer Pan, Eric Cousineau, Benjamin Burchfiel, Siyuan Feng, Russ Tedrake, and Shuran Song. Universal manipulation interface: In-the-wild robot teaching without in-the-wild robots. *arXiv preprint arXiv:2402.10329*, 2024.

[7] OX-Embodiment Collaboration, Abby O'Neill, Abdul Rehman, Abhinav Gupta, Abhiram Maddukuri, Abhishek Gupta, Abhishek Padalkar, Abraham Lee, Acorn Pooley, Agrim Gupta, et al. Open x-embodiment: Robotic learning datasets and rt-x models. *arXiv preprint arXiv:2310.08864*, 1(2), 2023.

[8] Yifan Ye, Yankai Fu, Yaoxu Lv, Bohan Hou, Jun Cen, Lingdong Kong, Duo Zheng, Tianxing Chen, Jiaming Liu, Ziang Cao, et al. Data pyramid for embodied manipulation: a survey. *arXiv preprint arXiv:2607.24744*, 2026.

[9] Fangcheng Liu, Yeqing Shen, Anda Cheng, Weishi Mi, Chao Tang, Chenyuan Liu, Yushun Xiang, Tingguang Li, Yong-Lu Li, and Yehui Tang. Roboicl: Embodied in-context learning with gpt-6 astra. *arXiv preprint arXiv:2609.34261*, 2026.

[10] Dongzhou Cheng, Taoran Yi, Ye Fang, Xingwu Zhang, Fan Feng, Yixuan Li, Gengxiong Zhuang, Rongze Wang, Shuai Yang, Wei Song, et al. In-context robot learning with vlm agents. *arXiv preprint arXiv:2609.19138*, 2026.

[11] Zhirui Fang, Qingchi Yu, Ziyang Chen, Longfei Li, Haoran Ma, Keru Zhou, Xinrun Xu, Samith Va, Yuxuan Hu, Peixuan Song, et al. Emerge-policy: A robot mind emerges beyond a single policy. *arXiv preprint arXiv:2608.29896*, 2026.

[12] Hung-Jen Chen, Yu-Hsun Hou, Yan-Hong Chen, Yan-Fu Chen, Binghua Cai, Min Sun, and Chun-Yi Lee. When instructions retrieve trajectories: Diagnosing and mitigating generalization failures in VLA models. *arXiv preprint arXiv:2609.39971*, 2026.

[13] Yu Fang, Yuchun Feng, Dong Jing, Jiaqi Liu, Yue Yang, Zhenyu Wei, Daniel Szafir, and Mingyu Ding. When vision overrides language: Evaluating and mitigating counterfactual failures in VLAs. Project website.

[14] Haochen Zhang and Yonatan Bisk. Flatness preserves instruction following in vision-language-action models. *arXiv preprint arXiv:2606.23641*, 2026.

[15] Yucheng Hu, Yanjiang Guo, Pengchao Wang, Xiaoyu Chen, Yen-Jen Wang, Jianke Zhang, Koushil Sreenath, Chaochao Lu, and Jianyu Chen. Video Prediction Policy: A Generalist Robot Policy with Predictive Visual Representations. *arXiv preprint arXiv:2412.14803*, 2024.

[16] Yue Liao, Pengfei Zhou, Siyuan Huang, Donglin Yang, Shengcong Chen, Yuxin Jiang, Yue Hu, Si Liu, Jianlan Luo, Liliang Chen, et al. Genie Envisioner: A Unified World Foundation Platform for Robotic Manipulation. In *International Conference on Learning Representations*, volume 2026, pages 88446–88463, 2026.

[17] Renhang Liu, Wenzhi Zhao, Zhuo Yang, Liliang Chen, Pengfei Zhou, Shengcong Chen, Guanghui Ren, Youlun Peng, Rongjun Jin, Nan Wang, et al. GE-Act 2.0: Pretraining and Scaling a World-Action Model for Robotic Manipulation. *arXiv preprint arXiv:2609.05588*, 2026.

[18] Shangchen Miao, Ningya Feng, Jialong Wu, Ye Lin, Xu He, Dong Li, and Mingsheng Long. JEPA-VLA: Video Predictive Embedding is Needed for VLA Models. *arXiv preprint arXiv:2602.11832*, 2026.

[19] Jiayi Chen, Wenxuan Song, Jingbo Wang, Shuai Zhou, Xicheng Gong, Zehua Fan, Ziyang Zhou, Haodong Yan, Fuhao Li, Qize Yu, et al. UniWAM: Unified World-Action Model. *arXiv preprint arXiv:2610.02054*, 2026.

[20] Simar Kareer, Karl Pertsch, James Darpinian, Judy Hoffman, Danfei Xu, Sergey Levine, Chelsea Finn, and Suraj Nair. Emergence of Human to Robot Transfer in Vision-Language-Action Models. *arXiv preprint arXiv:2512.22414*, 2025.

[21] Seonghyeon Ye, Yunhao Ge, Kaiyuan Zheng, Shenyuan Gao, Sihyun Yu, George Kurian, Suneel Indupuru, You Liang Tan, Chuning Zhu, Jiannan Xiang, et al. World Action Models are Zero-shot Policies. *arXiv preprint arXiv:2602.15922*, 2026.

[22] Zhihao Sun, Liu Liu, Xinjiang Wang, Haoyi Jiang, Wei Feng, Huiqiang Zhang, Xiaosong Jia, Zhizhong Su, and Zuxuan Wu. Ego4WAM: What Matters When Scaling Egocentric Human Data for Robot Learning? *arXiv preprint arXiv:2609.40341*, 2026.

[23] Bo Liu, Yifeng Zhu, Chongkai Gao, Yihao Feng, Qiang Liu, Yuke Zhu, and Peter Stone. LIBERO: Benchmarking Knowledge Transfer for Lifelong Robot Learning. *Advances in Neural Information Processing Systems*, 36:44776–44791, 2023.

[24] Senyu Fei, Siyin Wang, Junhao Shi, Zihao Dai, Jikun Cai, Pengfang Qian, Li Ji, Xinzhe He, Shiduo Zhang, Zhaoye Fei, et al. LIBERO-Plus: A Progressive Robustness Benchmark for Visual-Language-Action Models. In *Proceedings of the IEEE/CVF Conference on Computer Vision and Pattern Recognition*, pages 38574–38583, 2026.

[25] Tianxing Chen, Zanxin Chen, Baijun Chen, Zijian Cai, Yibin Liu, Zixuan Li, Qiwei Liang, Xianliang Lin, Yiheng Ge, Zhenyu Gu, et al. RoboTwin 2.0: A Scalable Data Generator and Benchmark with Strong Domain Randomization for Robust Bimanual Robotic Manipulation. *arXiv preprint arXiv:2506.18088*, 2025.

[26] Johan Bjorck, Fernando Castañeda, Nikita Cherniadev, Xingye Da, Runyu Ding, Linxi Fan, Yu Fang, Dieter Fox, Fengyuan Hu, Spencer Huang, et al. GR00T N1: An Open Foundation Model for Generalist Humanoid Robots. *arXiv preprint arXiv:2503.14734*, 2025.

[27] Gemini Robotics Team, Saminda Abeyruwan, Joshua Ainslie, Jean-Baptiste Alayrac, Montserrat Gonzalez Arenas, Travis Armstrong, Ashwin Balakrishna, Robert Baruch, Maria Bauza, Michiel Blokzijl, et al. Gemini Robotics: Bringing AI into the Physical World. *arXiv preprint arXiv:2503.20020*, 2025.

[28] Hongtao Wu, Ya Jing, Chilam Cheang, Guangzeng Chen, Jiafeng Xu, Xinghang Li, Minghuan Liu, Hang Li, and Tao Kong. Unleashing Large-Scale Video Generative Pre-training for Visual Robot Manipulation. In *International Conference on Learning Representations*, volume 2024, pages 10641–10662, 2024.

[29] Chi-Lam Cheang, Guangzeng Chen, Ya Jing, Tao Kong, Hang Li, Yifeng Li, Yuxiao Liu, Hongtao Wu, Jiafeng Xu, Yichu Yang, et al. GR-2: A Generative Video-Language-Action Model with Web-Scale Knowledge for Robot Manipulation. *arXiv preprint arXiv:2410.06158*, 2024.

[30] Team Wan, Ang Wang, Baole Ai, Bin Wen, Chaojie Mao, et al. Wan: Open and Advanced Large-Scale Video Generative Models. *arXiv preprint arXiv:2503.20314*, 2025.

[31] Niket Agarwal, Arslan Ali, Maciej Bala, Yogesh Balaji, Erik Barker, Tiffany Cai, Prithvijit Chattopadhyay, Yongxin Chen, Yin Cui, Yifan Ding, et al. Cosmos World Foundation Model Platform for Physical AI. *arXiv preprint arXiv:2501.03575*, 2025.

[32] Lin Li, Qihang Zhang, Yiming Luo, Shuai Yang, Ruilin Wang, Fei Han, Mingrui Yu, Zelin Gao, Nan Xue, Xing Zhu, et al. Causal World Modeling for Robot Control. *arXiv preprint arXiv:2601.21998*, 2026.

[33] Yanjiang Guo, Haodong Yan, Zhide Zhong, Zhongru Zhang, Qingyuan Yang, Qingzhou Lu, Xiaoyu Chen, Yen-Jen Wang, Shuying Deng, Chenghan Yang, et al. Video Prediction Policy 2: Predict Better, Act Better. *arXiv preprint arXiv:2610.10270*, 2026.

[34] Qihang Zhang, Lin Li, Luyao Zhang, Shuai Yang, Yiming Luo, Shuaiting Li, Ruilin Wang, Junke Wang, Jiahao Shao, Gangwei Xu, et al. Native Video-Action Pretraining for Generalizable Robot Control. *arXiv preprint arXiv:2607.08639*, 2026.

[35] Tianyuan Yuan, Zibin Dong, Yicheng Liu, and Hang Zhao. Fast-WAM: Do World Action Models Need Test-time Future Imagination? *arXiv preprint arXiv:2603.16666*, 2026.

[36] Shuang Li, Yihuai Gao, Dorsa Sadigh, and Shuran Song. Unified Video Action Model. *arXiv preprint arXiv:2503.00200*, 2025.

[37] Chuning Zhu, Raymond Yu, Siyuan Feng, Benjamin Burchfiel, Paarth Shah, and Abhishek Gupta. Unified World Models: Coupling Video and Action Diffusion for Pretraining on Large Robotic Datasets. *arXiv preprint arXiv:2504.02792*, 2025.

[38] Hongzhe Bi, Hengkai Tan, Shenghao Xie, Zeyuan Wang, Shuhe Huang, Haitian Liu, Ruowen Zhao, Yao Feng, Chendong Xiang, Yinze Rong, et al. Motus: A Unified Latent Action World Model. In *Proceedings of the IEEE/CVF Conference on Computer Vision and Pattern Recognition*, pages 35101–35113, 2026.

[39] Ruijie Zheng, Jing Wang, Scott Reed, Johan Bjorck, Yu Fang, Fengyuan Hu, Joel Jang, Kaushil Kundalia, Zongyu Lin, Loic Magne, et al. FLARE: Robot Learning with Implicit World Modeling. *arXiv preprint arXiv:2505.15659*, 2025.

[40] Jingwen Sun, Wenyao Zhang, Zekun Qi, Shaojie Ren, Zezhi Liu, Hanxin Zhu, Guangzhong Sun, Xin Jin, and Zhibo Chen. VLA-JEPA: Enhancing Vision-Language-Action Model with Latent World Model. In *European Conference on Computer Vision*, pages 478–497. Springer, 2026.

[41] Suraj Nair, Aravind Rajeswaran, Vikash Kumar, Chelsea Finn, and Abhinav Gupta. R3M: A Universal Visual Representation for Robot Manipulation. *arXiv preprint arXiv:2203.12601*, 2022.

[42] Yecheng Jason Ma, Shagun Sodhani, Dinesh Jayaraman, Osbert Bastani, Vikash Kumar, and Amy Zhang. VIP: Towards Universal Visual Reward and Representation via Value-Implicit Pre-Training. *arXiv preprint arXiv:2210.00030*, 2022.

[43] Ruihan Yang, Qinxi Yu, Yecheng Wu, Rui Yan, Borui Li, An-Chieh Cheng, Xueyan Zou, Yunhao Fang, Xuxin Cheng, Ri-Zhao Qiu, et al. EgoVLA: Learning Vision-Language-Action Models from Egocentric Human Videos. *arXiv preprint arXiv:2507.12440*, 2025.

[44] Ruijie Zheng, Dantong Niu, Yuqi Xie, Jing Wang, Mengda Xu, Yunfan Jiang, Fernando Castañeda, Fengyuan Hu, You Liang Tan, Letian Fu, et al. EgoScale: Scaling Dexterous Manipulation with Diverse Egocentric Human Data. *arXiv preprint arXiv:2602.16710*, 2026.

[45] Baoyu Li, Xinchen Yin, Mengying Lin, Yixin Zhang, and Danfei Xu. EgoWAM: World Action Models Beyond Pixels with In-the-Wild Egocentric Human Data. In *Robot World Models*, 2026.

[46] William Peebles and Saining Xie. Scalable Diffusion Models with Transformers. In *Proceedings of the IEEE/CVF International Conference on Computer Vision (ICCV)*, pages 4195–4205, 2023.

[47] Wan-Video. Wan2.2. Official code and model release, 2025. Released July 28, 2025; accessed October 22, 2026.

[48] Yaron Lipman, Ricky TQ Chen, Heli Ben-Hamu, Maximilian Nickel, and Matt Le. Flow Matching for Generative Modeling. *arXiv preprint arXiv:2210.02747*, 2022.

[49] Moo Jin Kim, Chelsea Finn, and Percy Liang. Fine-tuning vision-language-action models: Optimizing speed and success. *arXiv preprint arXiv:2502.19645*, 2025.

[50] Linqing Zhong, Yi Liu, Yifei Wei, Ziyu Xiong, Maoqing Yao, Si Liu, and Guanghui Ren. Acot-vla: Action chain-of-thought for vision-language-action models. *arXiv preprint arXiv:2601.11404*, 2026.

[51] Yihan Lin, Jiawei He, Shifeng Bao, Chen Zhao, Yang Li, Xiaobo Wang, Yan Wang, Cheng Chi, and Jing Zhang. Jepa-wam: Learning vision-language-action policies with joint-embedding world modeling. *arXiv preprint arXiv:2608.09381*, 2026.

[52] Ronghan Chen, Yandan Yang, Zuojin Tang, Dongjie Huo, Tong Lin, Haoning Wu, Haoyun Liu, Yuzhi Chen, Lulu Zheng, Botai Yuan, Tianlun Li, Mingxin Wang, Dekang Qi, Bin Hu, Wei Mei, Yuze Xuan, Haolong Yang, Yanqing Zhu, Mu Xu, Zhiheng Ma, and Xinyuan Chang. Abot-m0.5: Unified mobility-and-manipulation world action model. *arXiv preprint arXiv:2607.00678*, 2026.

[53] Hao Luo, Wanpeng Zhang, Yicheng Feng, Sipeng Zheng, Haiweng Xu, Chaoyi Xu, Ziheng Xi, Yuhui Fu, and Zongqing Lu. Being-H0.7: A Latent World-Action Model from Egocentric Videos. *arXiv preprint arXiv:2605.00078*, 2026.

[54] Moo Jin Kim, Yihuai Gao, Tsung-Yi Lin, Yen-Chen Lin, Yunhao Ge, Grace Lam, Percy Liang, Shuran Song, Ming-Yu Liu, Chelsea Finn, et al. Cosmos Policy: Fine-Tuning Video Models for Visuomotor Control and Planning. *arXiv preprint arXiv:2601.16163*, 2026.

[55] Haisheng Su, Zongdai Liu, Xin Jin, Haoxuan Dou, Chengming Hu, Baorun Li, Zhanwang Liu, Ruiyan Xu, Jianjie Fang, Xin Zhang, Zhenjie Yang, Xue Yang, Chen Gao, Junchi Yan, Yong Li, and Wei Wu. Worldscape policy 2.0: Empowering steerable world action modeling with reasoning-augmented memory and in-context learning. *arXiv preprint arXiv:2607.18840*, 2026.

[56] Lishan Yang, Wenxuan Song, Xi Wang, Pingyue Sheng, Zheng Fang, Ziyang Zhou, Junjie He, Haodong Yan, Jiayi Chen, Nan Sun, Qiao Sun, Pengwei Wang, Lingqiao Liu, Yan Wang, Yuxiang Gao, Feras Dayoub, and Haoang Li. 4d-wam: Infusing spatiotemporal awareness into world action models through trajectory fields. *arXiv preprint arXiv:2608.08023*, 2026.

[57] Jun Guo, Qiwei Li, Peiyan Li, Zilong Chen, Nan Sun, Yifei Su, Heyun Wang, Yuan Zhang, Xinghang Li, and Huaping Liu. Unified 4d world action modeling from video priors with asynchronous denoising. *arXiv preprint arXiv:2604.26694*, 2026.

[58] Yandan Yang, Shuang Zeng, Tong Lin, Xinyuan Chang, Dekang Qi, Junjin Xiao, Haoyun Liu, Ronghan Chen, Yuzhi Chen, Dongjie Huo, Feng Xiong, Xing Wei, Zhiheng Ma, and Mu Xu. Abot-m0: Vla foundation model for robotic manipulation with action manifold learning. *arXiv preprint arXiv:2602.11236*, 2026.

[59] StarVLA Community. Starvla: A lego-like codebase for vision-language-action model developing. *arXiv preprint arXiv:2604.05014*, 2026.

[60] Galaxea Team. Galaxea g0: Open-world dataset and dual-system vla model. *arXiv preprint arXiv:2509.00576*, 2025.